The few body problem of the quark-model hadron structure

A. Valcarce and T.F. Caramés

Departamento de Física Fundamental,
Universidad de Salamanca, E-37008 Salamanca, Spain

J. Vijande

Departamento de Física Atómica, Molecular y Nuclear,
Universidad de Valencia (UV) and IFIC (UV-CSIC), Valencia, Spain.

H. Garcilazo

Escuela Superior de Física y Matemáticas,
Instituto Politécnico Nacional, Edificio 9, 07738 México D.F., Mexico

(Dated: December 22, 2010)

Abstract

We discuss recent results of hadron spectroscopy and hadron-hadron interaction within a quark model framework. New experimental data could point to the important role played by higher order Fock space components on low-energy observables. Our aim is to obtain a coherent description of the low-energy hadron phenomenology to constrain QCD phenomenological models and try to learn about low-energy realizations of the theory. This long-range effort is based in adapting few-body techniques to study many-quark systems.

PACS numbers:

I. INTRODUCTION

The last decade has been especially challenging for hadron structure. New experimental data have shaken our understanding of QCD low-energy phenomenology. This earthquake had its epicenter on charmonium spectroscopy. Since Gell-Mann conjecture, most of the meson experimental data were classified as $q\bar{q}$ states according to $SU(N)$ irreducible representations. Its simplicity had converted meson spectroscopy in an ideal system to learn about the properties of QCD. Nevertheless a number of interesting issues remain still open as for example the understanding of some D-meson data obtained on the B factories or the structure of the scalar mesons. Some of the D_s states can be hardly accommodated in a pure $q\bar{q}$ description. They present a mass much lower than the naïve prediction of constituent quark models. Besides, the underlying structure of the scalar mesons is still not well established theoretically. These discrepancies gave rise to the hypothesis about possible contributions of higher order Fock space components allowed by the Gell-Mann classification. These ideas were simultaneously extended to the baryon sector, enlightening some of the obscure remaining problems.

In this talk we give an overview of the old dream of getting a coherent understanding of the low-energy hadron phenomenology [1]. We make emphasis on two different aspects. Firstly, we will address the study of meson and baryon spectroscopy in an enlarged Hilbert space considering four and five quark components. This seems nowadays unavoidable to understand the experimental data and it builds the bridge towards the description in terms of hadronic degrees of freedom. Secondly, the same scheme used to describe the hadron spectroscopy should be valid for describing the low-energy hadron-hadron scattering. We review our recent efforts to account for the strangeness -1 and -2 two- and three-baryon systems within the same scheme used for hadron spectroscopy and that has also demonstrated its validity for the nucleon-nucleon sector.

In particular we will address three different problems. In the first section we will discuss the charmonium spectroscopy above the threshold for the production of D mesons. The second section is devoted to study the effect of selected S-wave meson-baryon channels to match poor baryon mass predictions from quark models with data. Finally, the third section addresses the problem of the study of two- and three-baryon systems with strangeness -1 and -2 by means of a baryon-baryon interaction derived from the quark model used to study the hadron spectroscopy.

II. HEAVY MESONS: CHARMONIUM

Charmonium has been used as the test bed to demonstrate the color Fermi-Breit structure of quark atoms obeying the same principles as ordinary atoms [2]. Its nonrelativistic character ($v/c \approx 0.2 - 0.3$) gave rise to an amazing agreement between experiment and simple quark potential model predictions as $c\bar{c}$ states [3]. Close to the threshold for the production of charmed mesons quark-antiquark models required of an improved interaction [4]. The corrections introduced to the quark-antiquark spectra explained some deviations observed experimentally [5].

Since 2003, we have witnessed a growth of puzzling new charmonium mesons, like the well-established $X(3872)$ or the not so well-established $Y(4260)$, $Z(3930)$, $X(3940)$, $Y(3940)$, $X(4008)$, $X(4160)$, $X(4260)$, $Y(4350)$, and $Y(4660)$. In addition, the Belle Collaboration has reported the observation of similar states with non-zero electric charge: the $Z(4430)$,

the $Z_1(4040)$ and the $Z_2(4240)$ that have not yet been confirmed by other experiments [6].

These new states do not fit, in general, the simple predictions of the quark-antiquark schemes and, moreover, they overpopulate the expected number of states in (simple) two-body theories. This situation is not uncommon in particle physics. For example, in the light scalar-isoscalar meson sector hadronic molecules offer a reasonable explanation of the experimental data [7]. Also, the study of the NN system above the pion production threshold required new degrees of freedom to be incorporated in the theory, either as pions or as excited states of the nucleon, i.e., the Δ [8]. This discussion suggests that charmonium spectroscopy could be rather simple below the threshold production of charmed mesons but much more complex above it. In particular, the coupling to the closest $(c\bar{c})(n\bar{n})$ system, referred to as *unquenching the naïve quark model* [9], could be an important spectroscopic ingredient. Besides, hidden-charm four-quark states could explain the overpopulation of quark-antiquark theoretical states.

In an attempt to disentangle the role played by multiquark configurations in the charmonium spectroscopy we have solved the Lippmann-Schwinger equation for the scattering of two D mesons looking for attractive channels that may contain a meson-meson molecule [10]. In order to account for all basis states we allow for the coupling to charmonium-light two-meson systems. When we consider the system of two mesons M_1 and $\overline{M}_2$ ($M_i = D, D^*$) in a relative $S-$state interacting through a potential V that contains a tensor force then, in general, there is a coupling to the $M_1\overline{M}_2$ $D-$wave and the Lippmann-Schwinger equation of the system is

$$t_{ji}^{\ell s\ell'' s''}(p,p'';E) = V_{ji}^{\ell s\ell'' s''}(p,p'') + \sum_{\ell' s'} \int_0^\infty p'^2 dp'\, V_{ji}^{\ell s\ell' s'}(p,p') \frac{1}{E - p'^2/2\mu + i\epsilon} t_{ji}^{\ell' s'\ell'' s''}(p',p'';E), \tag{1}$$

where t is the two-body amplitude, j, i, and E are the angular momentum, isospin and energy of the system, and ℓs, $\ell' s'$, $\ell'' s''$ are the initial, intermediate, and final orbital angular momentum and spin; p and μ are the relative momentum and reduced mass of the two-body system, respectively. In the case of a two D meson system that can couple to a charmonium-light two-meson state, for example when $D\overline{D}^*$ is coupled to $J/\Psi\omega$, the Lippmann-Schwinger equation for $D\overline{D}^*$ scattering becomes

$$\begin{aligned} t_{\alpha\beta;ji}^{\ell_\alpha s_\alpha \ell_\beta s_\beta}(p_\alpha,p_\beta;E) = V_{\alpha\beta;ji}^{\ell_\alpha s_\alpha \ell_\beta s_\beta}(p_\alpha,p_\beta) \;&+\; \sum_\gamma \sum_{\ell_\gamma s_\gamma} \int_0^\infty p_\gamma^2 dp_\gamma V_{\alpha\gamma;ji}^{\ell_\alpha s_\alpha \ell_\gamma s_\gamma}(p_\alpha,p_\gamma) \\ &\times\; G_\gamma(E;p_\gamma) t_{\gamma\beta;ji}^{\ell_\gamma s_\gamma \ell_\beta s_\beta}(p_\gamma,p_\beta;E), \end{aligned} \tag{2}$$

with $\alpha,\beta,\gamma = D\overline{D}^*, J/\Psi\omega$.

We have consistently used the same interacting Hamiltonian to study the two- and four-quark systems to guarantee that thresholds and possible bound states are eigenstates of the same Hamiltonian. This study has been the first systematic analysis of four-quark hidden-charm meson-meson molecules. For the first time a consistent study of all quantum numbers within the same model was performed. Our predictions robustly show that no deeply bound states can be expected for this system. Only a few channels, see Table I, can be expected to present observable resonances or slightly bound states. Among them, we have found that the $D\overline{D}^*$ system must show a bound state slightly below threshold with quantum numbers $J^{PC}(I) = 1^{++}(0)$, that could correspond to the widely discussed $X(3872)$. This result is illustrated in Fig. 1. Out of the systems made of a particle and its corresponding antiparticle, $D\overline{D}$ and $D^*\overline{D}^*$, the $J^{PC}(I) = 0^{++}(0)$ is attractive. It would be

TABLE I: Attractive channels for the two $D-$meson systems.

System	$D\overline{D}$	$D\overline{D}^*$		$D^*\overline{D}^*$	
$J^{PC}(I)$	$0^{++}(0)$	$1^{++}(0)$	$0^{++}(0)$	$2^{++}(0)$	$2^{++}(1)$

the only candidate to accommodate a wide resonance for the $D\overline{D}$ system. For the $D^*\overline{D}^*$ the attraction is stronger and structures may be observed close and above the charmed meson production threshold. Also, we have shown that the $J^{PC}(I) = 2^{++}(0,1)$ $D^*\overline{D}^*$ channels are attractive due to the coupling to the $J/\Psi\omega$ and $J/\Psi\rho$ channels, respectively.

Among these exotic theoretical states, charged states have an unique feature: by construction they cannot be accommodated into the conventional $c\bar{c}$ spectrum. Two different experimental findings show positive results on charge charmonium mesons. The first one was a $\Psi(2S)\pi^+$ peak at about 4430 MeV/c^2 observed by Belle in the $\bar{B}^0 \to \Psi(2S)\pi^+K^-$ decays [11]. A second positive observation was reported by Belle from the $B^0 \to \Xi_{c1}\pi^+K^-$ decay, with two resonances in $\Xi_{c1}\pi^+$ at masses of about 4050 and 4250 MeV/c^2 [12]. In the first case, BaBar has presented its own analysis [13] performing a detailed study of the acceptance and possible reflections concluding that no significant signal exists on the data. While the two experiments made different conclusion, the data itself seem to be in a reasonable agreement except for the lower available statistics of the BaBar experiment. The states found in Ref. [12] could correspond to the $D^*\overline{D}^*$ $J^{PC}(I) = 2^{++}(1)$ we have predicted [14]. Its confirmation would represent a unique tool in discriminating among different theoretical models.

FIG. 1: Fredholm determinant for the $J^{PC}(I) = 1^{++}(0)$ $D\overline{D}^*$ system. Solid (dashed) line: results with (without) coupling to the $J/\Psi\omega$ channel.

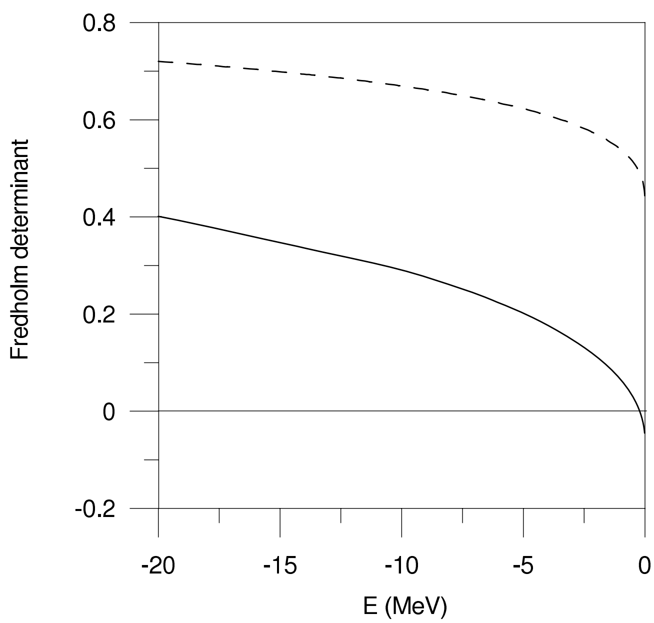

III. LIGHT BARYONS

As we have seen above, there is nowadays compelling evidence of meson resonances containing more than quark-antiquark ($q\overline{q}$) valence components. One can guess a similar situation for some baryon resonances that may contain more than three-quark ($3q$) valence components. In the baryon sector a paradigmatic case is the $\Lambda(1405)$ which requires the consideration of a $N\overline{K}$ component for its explanation. In the meson sector scalars such as the f_0's contain relevant meson-meson components. In all these cases valence quark models based on $3q$ or $q\overline{q}$ components that describe correctly the bulk of spectral data fail systematically to reproduce their masses. Actually we can interpret the systematic failure in the description of a given resonance by valence quark models as an indication of its anomalous nature in the sense of containing more than the valence components. Here we use this interpretation as a criteria to identify possible anomalies in the Light-quark Baryon Spectrum (LqBS).

A comparative analysis of Constituent Quark Models (CQM) predictions for the LqBS has been carried out in Ref. [15]. This analysis makes clear the presence of anomalies for which $3q$ predicted masses are significantly higher than their Particle Data Group (PDG) averages [16], see Fig. 2. Moreover all the anomalies have in common the existence of $S-$wave meson-baryon thresholds with the same quantum numbers than the anomalies (also drawn in Fig. 2) close above the PDG average masses. This suggests a possible contribution of these meson-baryon ($4q1\overline{q}$) components to the anomalies to give a correct account of their masses. To make a rough estimate of this contribution we shall consider the coupling of the free meson-baryon (mb) channels to the corresponding $3q$ states. To make effective such a

FIG. 2: Mass predictions for the anomalies from Ref. [17] (dashed lines) as compared to the experimental mass intervals (boxes). N.C. means non-cataloged resonance. Meson-baryon thresholds are indicated by solid lines.

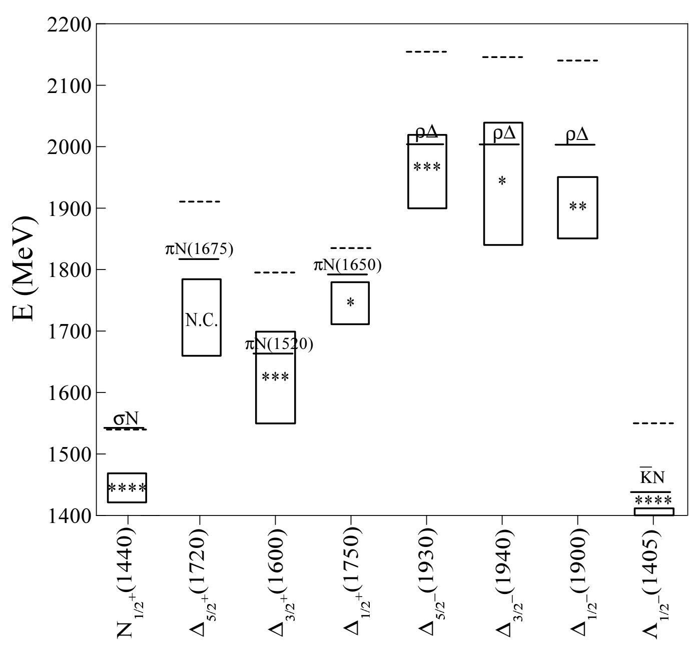

FIG. 3: Predicted masses for the anomalies (dashed lines) as compared to the experimental mass intervals (boxes). N.C. means non-cataloged resonance.

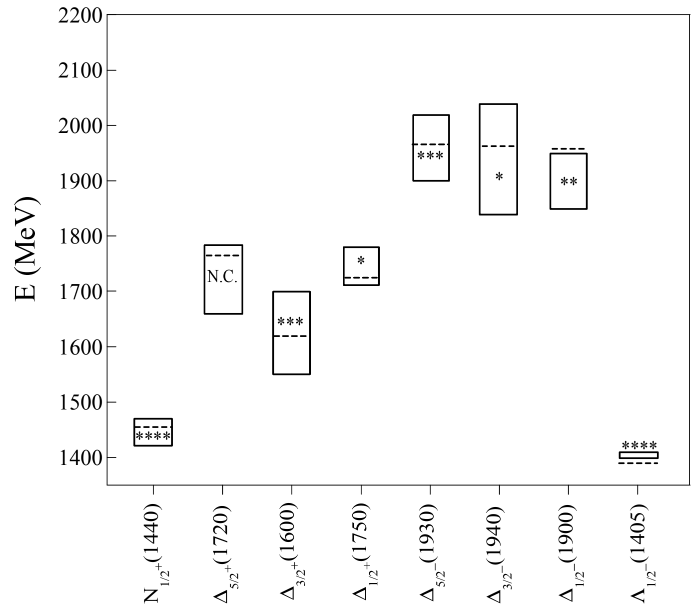

coupling we parametrize the transition matrix element, $< mb\,|H|\,3q >\equiv a$, and diagonalize the hamiltonian matrix by assuming $< 3q\,|H|\,3q >= M_{3q}$ being M_{3q} the predicted $3q$ mass and $< mb\,|H|\,mb >\sim M_m + M_b$ being $M_m + M_b$ the mass of the meson-baryon threshold. The results from the diagonalization corresponding to the lowest energy states are shown in Fig. 3. Despite the shortcomings of our toy model calculation the quantitative agreement with data is spectacular (there is only one universal parameter, a, assumed for simplicity to be the same in all cases). Qualitatively our toy model implies that the anomalies correspond mostly to meson-baryon states but with a non-negligible three-quark probability that makes them stable against decay into $m + b$. This interpretation could need some refinement when going to a more complete model where the meson-baryon interaction were also considered ($< mb\,|H|\,mb >\sim M_m + M_b$). Then some anomalies might appear as simply meson-baryon bound states. Keeping this in mind we may conclude that the coupling to selected mb channels acts as an effective healing mechanism to match deficient CQM predictions with data. Furthermore the implementation of these selected channels in the analyses of data might add certainty to the existence of the anomalies and at the same time help to reconcile competing and sometimes not compatible partial wave analyses. Indeed the incorporation of some of our effective inelastic mb channels in data analyses has been very relevant for the experimental extraction of the corresponding anomalies: σN for $N_{P_{11}}(1440)$ [18] and $\rho\Delta$ for $\Delta_{D_{35}}(1930)$ [18, 19].

IV. STRANGENESS -1 AND -2 TWO AND THREE-BARYON SYSTEMS

In this section, we review recent studies of two and three-baryon systems with strangeness -1 and -2 using two-body interactions derived from the quark model.

A. The two-body interactions

The baryon-baryon interactions are obtained from the chiral constituent quark model [1, 20]. In order to derive the local $B_1B_2 \to B_3B_4$ potentials from the basic qq interaction defined above we use a Born-Oppenheimer approximation. Explicitly, the potential is calculated as follows,

$$V_{B_1B_2(L\,S\,T)\to B_3B_4(L'\,S'\,T)}(R) = \xi_{L\,S\,T}^{L'\,S'\,T}(R) \, - \, \xi_{L\,S\,T}^{L'\,S'\,T}(\infty)\,, \tag{3}$$

where

$$\xi_{L\,S\,T}^{L'\,S'\,T}(R) \, = \, \frac{\left\langle \Psi_{B_3B_4}^{L'\,S'\,T}(\vec{R}) \mid \sum_{i<j=1}^{6} V_{qq}(\vec{r}_{ij}) \mid \Psi_{B_1B_2}^{L\,S\,T}(\vec{R}) \right\rangle}{\sqrt{\left\langle \Psi_{B_3B_4}^{L'\,S'\,T}(\vec{R}) \mid \Psi_{B_3B_4}^{L'\,S'\,T}(\vec{R}) \right\rangle}\sqrt{\left\langle \Psi_{B_1B_2}^{L\,S\,T}(\vec{R}) \mid \Psi_{B_1B_2}^{L\,S\,T}(\vec{R}) \right\rangle}}\,. \tag{4}$$

In the last expression the quark coordinates are integrated out keeping R fixed, the resulting interaction being a function of the $B_i - B_j$ relative distance. The wave function $\Psi_{B_iB_j}^{L\,S\,T}(\vec{R})$ for the two-baryon system is discussed in detail in Ref. [1].

In Ref. [21] we constructed different families of $S = -1$ interacting potentials, by introducing small variations of the mass of the effective scalar exchange potentials, that allow us to study the dependence of the results on the strength of the spin-singlet and spin-triplet hyperon-nucleon interactions. These potentials are characterized by the ΛN scattering lengths $a_{i,s}$ and they reproduce the cross sections near threshold of the five hyperon-nucleon processes for which data are available (see Ref. [21]). Let us analyze the three-body systems with strangeness -1.

B. The ΛNN system

The channels (I, J) = (0,1/2) and (0,3/2) are the most attractive ones of the ΛNN system. In particular, the channel (0,1/2) has the only bound state of this system, the hypertriton. We give in Table II the results of the models constructed in Ref. [21] for the two Λd scattering lengths and the hypertriton binding energy. We compare with the results,

TABLE II: Λd scattering lengths, $A_{0,3/2}$ and $A_{0,1/2}$ (in fm), and hypertriton binding energy, $B_{0,1/2}$ (in MeV), for several hyperon-nucleon interactions characterized by ΛN scattering lengths $a_{1/2,0}$ and $a_{1/2,1}$ (in fm).

$a_{1/2,0}$	$a_{1/2,1}$	$A_{0,3/2}$	$A_{0,1/2}$	$B_{0,1/2}$
2.48	1.41	31.9 (66.3)	−16.0 (−20.0)	0.129 (0.089)
2.48	1.65	−72.8 (198.2)	−13.8 (−17.2)	0.178 (0.124)
2.48	1.72	−40.8 (−179.8)	−13.3 (−16.6)	0.192 (0.134)
2.48	1.79	−28.5 (−62.7)	−12.9 (−16.0)	0.207 (0.145)
2.48	1.87	−22.0 (−38.2)	−12.5 (−15.4)	0.223 (0.156)
2.48	1.95	−17.9 (−27.6)	−12.1 (−14.9)	0.239 (0.168)
2.31	1.65	−76.0 (198.2)	−17.1 (−22.4)	0.113 (0.070)
2.55	1.65	−73.6 (198.2)	−13.6 (−16.8)	0.185 (0.130)
2.74	1.65	−72.1 (198.2)	−12.0 (−14.4)	0.244 (0.182)

TABLE III: Hypertriton binding energy (in MeV) for several hyperon-nucleon interactions characterized by ΛN scattering lengths $a_{1/2,0}$ and $a_{1/2,1}$ (in fm) which are within the experimental error bars $B_{0,1/2} = 0.130 \pm 0.050$ MeV.

	$a_{1/2,1} = 1.41$	$a_{1/2,1} = 1.46$	$a_{1/2,1} = 1.52$	$a_{1/2,1} = 1.58$
$a_{1/2,0} = 2.33$	0.080	0.087	0.096	0.106
$a_{1/2,0} = 2.39$	0.094	0.102	0.112	0.122
$a_{1/2,0} = 2.48$	0.129	0.140	0.152	0.164

in parentheses, obtained in Ref. [21] including only the three-body S wave configurations. As a consequence of considering the D waves, the hypertriton binding energy increases by about 50−60 keV [23], while the $A_{0,1/2}$ scattering length decreases by about 3−5 fm. The largest changes occur in the $A_{0,3/2}$ scattering length where both positive and negative values appeared which means, in the case of the negative values, that a bound state is generated in the $(I, J) = (0, 3/2)$ channel. Since this channel depends mainly on the spin-triplet hyperon-nucleon interaction and experimentally there is no evidence whatsoever for the existence of a $(I, J) = (0, 3/2)$ bound state one can use the results of this channel to set limits on the value of the hyperon-nucleon spin-triplet scattering length $a_{1/2,1}$. As one can guess from Table II, the three-body channel $(I, J) = (0, 3/2)$ becomes bound if $a_{1/2,1} > 1.58$ fm (see Ref. [22]. Moreover, we found in Ref. [21] that the fit of the hyperon-nucleon cross sections is worsened for those cases where the spin-triplet ΛN scattering length is smaller than 1.41 fm, so that we conclude that $1.41 \leq a_{1/2,1} \leq 1.58$ fm. To set some limits to the hyperon-nucleon spin-singlet scattering length, we have calculated in Table III the hypertriton binding energy using for the hyperon-nucleon spin-triplet scattering length the allowed values $1.41 \leq a_{1/2,1} \leq 1.58$ fm and for the spin-singlet scattering length $2.33 \leq a_{1/2,0} \leq 2.48$ fm which leads to results for the hypertriton binding energy within the experimental error bars $B_{0,1/2} = 0.13 \pm 0.05$ MeV.

With regard to the isospin 1 channels $(I, J) = (1, 1/2)$ and $(1, 3/2)$, the $(1, 1/2)$ channel is attractive but not enough to produce a bound state while the $(1, 3/2)$ channel is repulsive.

TABLE IV: Σd scattering lengths, $A'_{1,3/2}$ and $A'_{1,1/2}$ (in fm), and position of the quasibound state $B'_{1,1/2}$ (in MeV) for several hyperon-nucleon interactions characterized by ΛN scattering lengths $a_{1/2,0}$ and $a_{1/2,1}$ (in fm).

$a_{1/2,0}$	$a_{1/2,1}$	$A'_{1,3/2}$	$A'_{1,1/2}$	$B'_{1,1/2}$
2.48	1.41	$0.14+i\,0.24$ $(0.20+i\,0.26)$	$19.82+i\,16.94$ $(19.28+i\,25.37)$	$2.92-i\,2.17$
2.48	1.65	$0.28+i\,0.27$ $(0.36+i\,0.29)$	$12.08+i\,38.98$ $(-1.55+i\,42.31)$	$2.84-i\,2.14$
2.48	1.72	$0.32+i\,0.28$ $(0.40+i\,0.30)$	$2.92+i\,43.20$ $(-10.47+i\,40.25)$	$2.82-i\,2.11$
2.48	1.79	$0.36+i\,0.29$ $(0.44+i\,0.31)$	$-8.00+i\,42.58$ $(-17.33+i\,35.01)$	$2.79-i\,2.10$
2.48	1.87	$0.40+i\,0.30$ $(0.49+i\,0.33)$	$-16.90+i\,37.08$ $(-21.16+i\,28.54)$	$2.77-i\,2.09$
2.48	1.95	$0.45+i\,0.31$ $(0.54+i\,0.34)$	$-21.73+i\,29.48$ $(-22.44+i\,22.44)$	$2.75-i\,2.08$
2.31	1.65	$0.28+i\,0.27$ $(0.36+i\,0.29)$	$19.01+i\,23.21$ $(14.95+i\,31.61)$	$2.88-i\,2.14$
2.55	1.65	$0.28+i\,0.27$ $(0.36+i\,0.29)$	$-12.81+i\,43.49$ $(-21.04+i\,33.19)$	$2.79-i\,2.11$
2.74	1.65	$0.28+i\,0.27$ $(0.36+i\,0.29)$	$-26.01+i\,17.95$ $(-23.29+i\,13.32)$	$2.73-i\,2.09$

FIG. 4: Real and imaginary parts of the Σd scattering length $A'_{1,1/2}$ as a function of the ΛN $a_{1/2,1}$ scattering length.

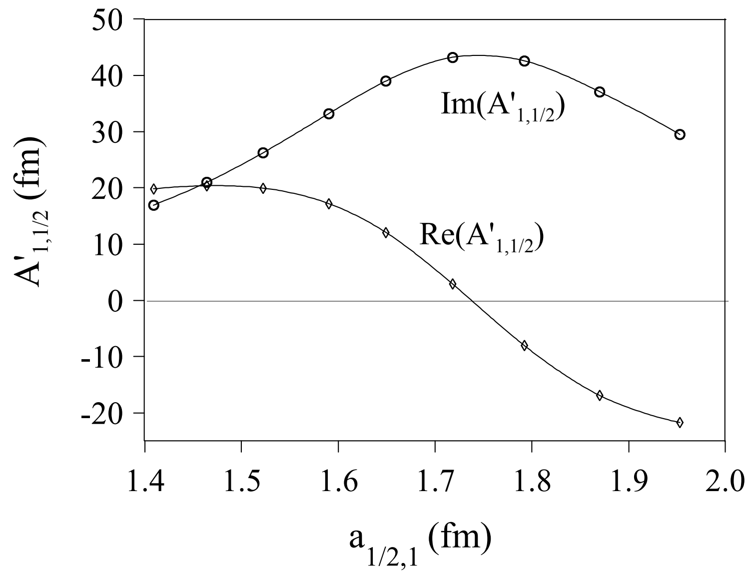

C. The ΣNN system

We show in Table IV the Σd scattering lengths $A'_{1,3/2}$ and $A'_{1,1/2}$. The Σd scattering lengths are complex since the inelastic ΛNN channels are always open. The scattering length $A'_{1,3/2}$ depends mainly on the spin-triplet hyperon-nucleon channels and both its real and imaginary parts increase when the spin-triplet hyperon-nucleon scattering length increases. The effect of the three-body D waves is to lower the real part by about 20 % and the imaginary part by about 10 %. The scattering length $A'_{1,1/2}$ shows large variations between the results with and without three-body D waves but this is due, as we will see next, to the fact that there is a pole very near threshold, a situation quite similar to that of the $A_{0,3/2}$ Λd scattering length discussed in the previous subsection.

We plot in Fig. 4 the real and imaginary parts of the Σd scattering length $A'_{1,1/2}$ as functions of the spin-triplet ΛN scattering length $a_{1/2,1}$, since by increasing $a_{1/2,1}$ one is increasing the amount of attraction that is present in the three-body channel. As one can see, Re($A'_{1,1/2}$) changes sign from positive to negative while at the same time Im($A'_{1,1/2}$) has a maximum. These two features are the typical ones that signal that the channel has a quasibound state [24]. The position of this pole in the complex plane, which is given in the last column of Table IV, changes very little with the model used and it lies at around $2.8 - i\,2.1$ MeV.

D. Strangeness -2 two-baryon systems

The knowledge of the strangeness $S = -2$ two-baryon interactions has become an important issue for theoretical and experimental studies of the strangeness nuclear physics. Moreover, this is an important piece of a more fundamental problem, the description of the interaction of the different members of the baryon octet in a unified way. The $\Xi N - \Lambda\Lambda$ interaction accounts for the existence of doubly strange hypernuclei, which is a gateway

to strange hadronic matter. Strangeness -2 baryon-baryon interactions also account for a possible six-quark H-dibaryon, which has yet to be experimentally observed.

There has been a steady progress towards the $S = -2$ baryon-baryon interaction. The ΛN interaction is pretty much understood based on the experimental data of Λ hypernuclei. There is also some progress made on the ΣN interaction. However, the experimental knowledge on the ΞN and hyperon-hyperon (YY) interactions is quite poor. The only information available came from doubly strange hypernuclei, suggesting that the $^1S_0$ $\Lambda\Lambda$ interaction should be moderately attractive. An upper limit of $B_{\Lambda\Lambda} = 7.25 \pm 0.19$ MeV has been deduced for a hypothetical H-dibaryon (a lower limit of 2223.7 MeV/c^2 for its mass) from the so-called Nagara event [25] at a 90% confidence level. The KEK-E176/E373 hybrid emulsion experiments observed other events corresponding to double$-\Lambda$ hypernuclei. Among them, the Demachi-Yanagi [26, 27], identified as $^{10}_{\Lambda\Lambda}$Be drove a value of $B_{\Lambda\Lambda} = 11.90 \pm 0.13$ [28]. A new observed double-Λ event has been recently reported by the KEK-E373 experiment, the Hida event [27], although with uncertainties on its nature it has been interpreted as an observation of the ground state of the $^{11}_{\Lambda\Lambda}$Be [28]. Very recently, doubly strange baryon-baryon scattering data at low energies were deduced for the first time, obtaining some experimental data and upper limits for different elastic and inelastic cross sections: $\Xi^- p \to \Xi^- p$ and $\Xi^- p \to \Lambda\Lambda$ [29]. Recent results of the KEK-PS E522 experiment indicate the possibility of a H-dibaryon as a resonance state with a mass range between the $\Lambda\Lambda$ and $N\Xi$ thresholds [30].

In the planned experiments at J-PARC [31], dozens of emulsions events for double$-\Lambda$ hypernuclei will be produced. The (K^-, K^+) reaction is one of the most promising ways of studying doubly strange systems. $\Lambda\Lambda$ hypernuclei can be produced through the reaction $K^- p \to K^+ \Xi^-$ followed by $\Xi^- p \to \Lambda\Lambda$. It is therefore compulsory having theoretical predictions concerning the $\Xi N - \Lambda\Lambda$ coupling [32] to guide the experimental way and, in a symbiotic manner, to use the new experimental data as a feedback of our theoretical knowledge.

In this section, we derive the strangeness -2 baryon-baryon interactions: $\Lambda\Lambda$, $\Lambda\Sigma$, $\Sigma\Sigma$ and $N\Xi$. We use these two-body interactions to calculate two-body elastic and inelastic scattering cross sections [33] and we compare to experimental data and other theoretical models. We also calculate the two-body scattering lengths of the different spin-isospin channels to compare with other theoretical models. We show in Fig. 5 the $\Xi^- p$ elastic cross section compared to the in-medium experimental $\Xi^- p$ cross section around $p^{\Xi}_{\rm lab} = 550$ MeV/c, where $\sigma_{\Xi^- p} = 30 \pm 6.7\ ^{+3.7}_{-3.6}$ mb [34]. Another analysis using the eikonal approximation gives $\sigma_{\Xi^- p} = 20.9 \pm 4.5\ ^{+2.5}_{-2.4}$ mb [35]. A more recent experimental analysis [29] for the low energy $\Xi^- p$ elastic and $\Xi^- p \to \Lambda\Lambda$ total cross sections in the range 0.2 GeV/c to 0.8 GeV/c shows that the former is less than 24 mb at 90% confidence level and the latter of the order of several mb, respectively. In Fig. 6 we present the inelastic $\Xi^- p \to \Lambda\Lambda$ cross section. It has been recently estimated at a laboratory momentum of $p^{\Xi}_{\rm lab} = 500$ MeV/c, see Ref. [29], assuming a quasifree scattering process for the reaction ^{12}C$(\Xi^-, \Lambda\Lambda)X$ obtaining a total cross section $\sigma(\Xi^- p \to \Lambda\Lambda) = 4.3^{+6.3}_{-2.7}$ mb. The upper limit of the cross section was derived as 12 mb at 90% confidence level. Fig. 7 shows the total inelastic cross section $\Xi^- p \to \Xi^0 n$. Combining the results of Refs. [29] and [36], one obtains $\sigma(\Xi^- p \to \Xi^0 n) \sim 10$ mb. A recent measurement of a quasifree $p(K^-, K^+)\Xi^-$ reaction in emulsion plates yielded $12.7^{+3.5}_{-3.1}$ mb for the total inelastic cross section in the momentum range $0.4 - 0.6$ GeV/c [37], consistent with the results of Ref. [36]. The experimental results for $\Xi^- p$ inelastic scattering of Refs. [36, 37] involve both $\Xi^- p \to \Lambda\Lambda$ and $\Xi^- p \to \Xi^0 n$ [29], what combined with the value for $\Xi^- p \to \Lambda\Lambda$ of Ref. [29] allows to obtain an estimate of the inelastic cross section $\Xi^- p \to \Xi^0 n$.

FIG. 5: $\Xi^- p$ elastic cross section, in mb, as a function of the laboratory Ξ momentum, in GeV/c. The two experimental data are taken from Ref. [34], black circle, and Ref. [35], black square (both are in-medium experimental data). The horizontal line indicates an upper limit for the cross section extracted in Ref. [29] with a large uncertainty in the momentum.

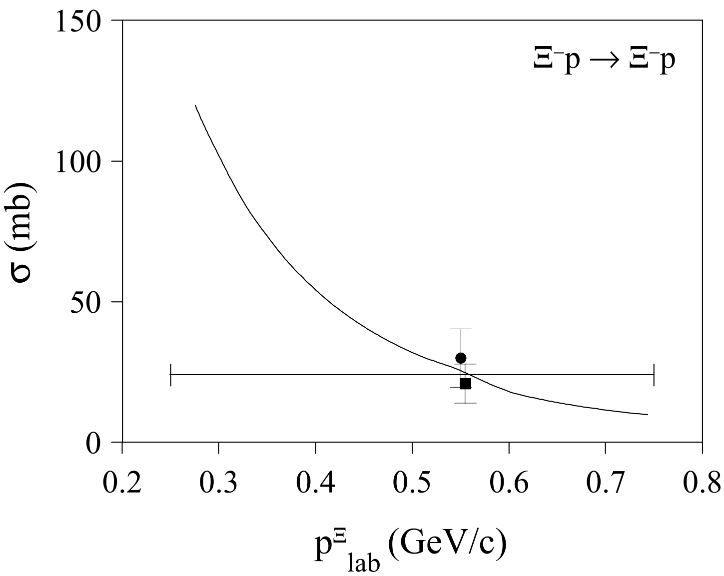

As can be seen our results agree with the experimental data for the elastic and inelastic ΞN cross sections. The small bumps in the cross sections correspond to the opening of inelastic channels. We would like to emphasize the agreement of our results with the $\Xi^- p \to \Lambda\Lambda$ conversion cross section. This reaction is of particular importance in assessing the stability of Ξ^- quasi-particle states in nuclei. Our results are close to the estimations of

FIG. 6: $\Xi^- p \to \Lambda\Lambda$ cross section, in mb, as a function of the laboratory Ξ momentum, in GeV/c. The experimental data is taken from Ref. [29].

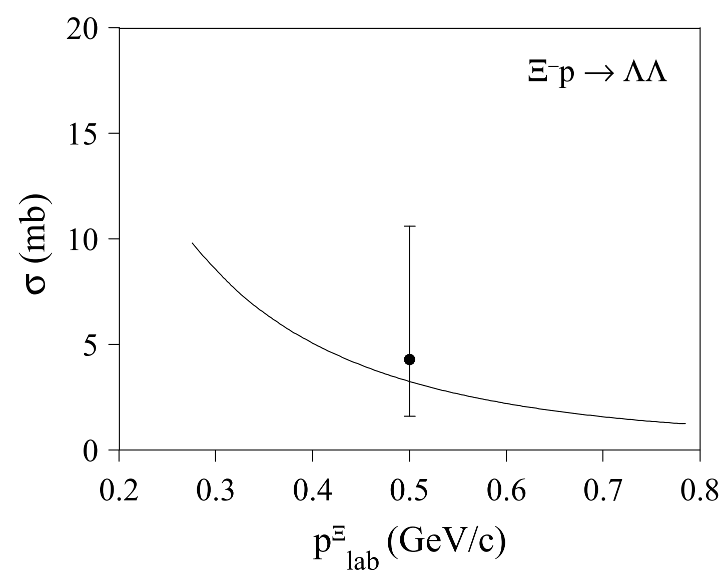

TABLE V: Two-body singlet and triplet scattering lengths, in fm, for different models as compared to our results. The results between squared brackets indicate the lower and upper limit for different parametrizations used in that reference.

Model	Ref. [40]	Ref. [41]	Ref. [39]	Ref. [23]	Ours [33]
$a^{\Lambda\Lambda}_{^1S_0}$	$[-0.27, -0.35]$	$[-1.555, -3.804]$	$[-1.52, -1.67]$	-0.821	-2.54
$a^{\Xi^0 p}_{^1S_0}$	$[0.40, 0.46]$	$[0.144, 0.491]$	$[0.13, 0.21]$	0.324	-3.32
$a^{\Xi^0 p}_{^3S_1}$	$[-0.030, 0.050]$	–	$[0.0, 0.03]$	-0.207	18.69
$a^{\Sigma^+\Sigma^+}_{^1S_0}$	$[6.98, 10.32]$	–	$[-6.23, -9.27]$	-85.3	0.523
$a^{\Xi N(I=0)}_{^1S_0}$	–	–	–	–	$-1.20 + i\,0.75$
$a^{\Xi N(I=0)}_{^3S_1}$	–	$[-1.672, 122.5]$	–	–	0.28
$a^{\Lambda\Sigma}_{^1S_0}$	–	–	–	–	$0.908 + i\,1.319$
$a^{\Lambda\Sigma}_{^3S_1}$	–	–	–	–	$-\,3.116 + i\,0.393$
$a^{\Sigma\Sigma(I=1)}_{^3S_1}$	–	–	–	–	$-\,1.347 + i\,1.801$
$a^{\Sigma\Sigma(I=0)}_{^1S_0}$	–	–	–	–	$-\,0.039 + i\,0.517$

the Nijmegen-D model [38]. Ref. [23] predicts $\sigma(\Xi^- p \to \Xi^0 n) \sim 15$ mb at $p^{\Xi}_{\rm lab} = 0.5$ GeV/c. Ref. [36] reported 14 mb for the inelastic scattering involving both $\Xi^- p \to \Lambda\Lambda$ and $\Xi^- p \to \Xi^0 n$. We found a smaller value of approximately 6 mb for both inelastic channels, in close agreement to experiment.

The scattering lengths for the different spin-isospin channels are given in Table V. These parameters are complex for the $N\Xi$ $(i, j) = (0, 0)$ since the inelastic $\Lambda\Lambda$ channel is open, for the $\Lambda\Sigma$ isospin 1 channel due to the opening of the $N\Xi$ channel, and for the $\Sigma\Sigma$ i =0 and 1 since the $\Lambda\Lambda$ and $N\Xi$ channels are open in the first case, and the $N\Xi$ and $\Lambda\Sigma$

FIG. 7: $\Xi^- p \to \Xi^0 n$ cross section, in mb, as a function of the laboratory Ξ momentum, in GeV/c. The experimental data are taken from Ref. [29] as explained in the text.

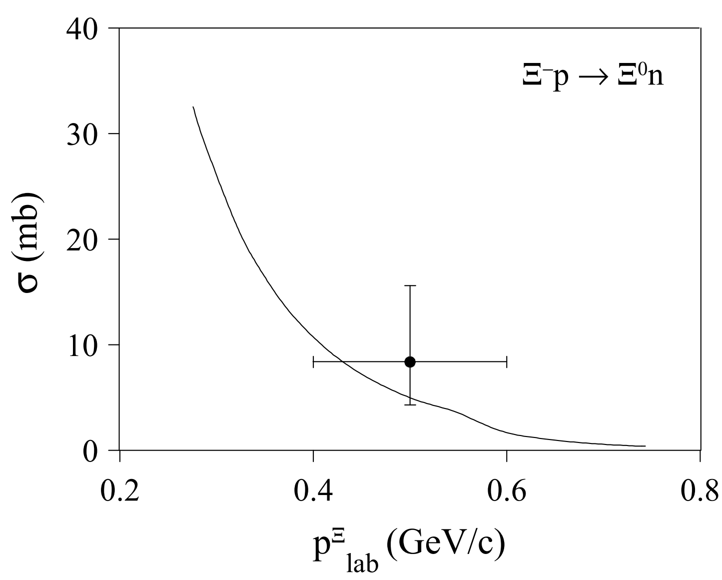

are open in the second. There is no direct comparison between our results and those of Ref. [23]. Although both are quark-model based results, Ref. [23] used an old-fashioned quark-model interacting potential. For example, they use a huge strong coupling constant, $\alpha_S = 1.9759$, and they consider the contribution of vector mesons what could give rise to double counting problems [42]. As explicitly written in Ref. [23], the parameters are effective in their approach and has very little to do with QCD. As mentioned above, since the observation of the Nagara event [25] it is generally accepted that the $\Lambda\Lambda$ interaction is only moderately attractive. Our result for the ${}^1S_0$ $\Lambda\Lambda$ scattering length is compatible with such event. A rough estimate of $B_{\Lambda\Lambda}(B_{\Lambda\Lambda} \approx (\hbar c)^2/2\mu_{\Lambda\Lambda}a^{\Lambda\Lambda}_{{}^1S_0})$ drives a value of 5.41 MeV, below the upper limit extracted from the Nagara event, $B_{\Lambda\Lambda} = 7.25 \pm 0.19$ MeV. Moreover, although from the $\Lambda\Lambda$ scattering length alone one cannot draw any conclusion on the magnitude of the two-Λ separation energy, recent estimates [43] have reproduced the two-Λ separation energy, defined as $\Delta B_{\Lambda\Lambda} = B_{\Lambda\Lambda}({}^{6}_{\Lambda\Lambda}\mathrm{He}) - 2B_{\Lambda}({}^{5}_{\Lambda}\mathrm{He})$, with scattering lengths of -1.32 fm.

V. SUMMARY

To summarize, we have reviewed some recent results of hadron spectroscopy and hadron-hadron interaction in terms of the constituent quark model. The main goal of our presentation was to highlight the complementarity of a simultaneous study of both problems in order to constrain low-energy realizations of the underlying theory, QCD. We have seen how the enlargement of the Hilbert space when increasing energy, that was seen to be necessary to describe the nucleon-nucleon phenomenology above the pion production threshold, seems to be necessary to understand current problems of hadron spectroscopy. We have also tried to emphasize that spectroscopy and interaction can and must be understood within the same scheme when dealing with quark models. Any other alternative becomes irrelevant from the point of view of learning about properties of QCD.

In our analysis we have shown the first systematic study of four-quark hidden-charm states as meson-meson molecules. For the first time a consistent study of all quantum numbers within the same model has been done. Our predictions robustly show that no deeply bound states can be expected for charmonium. Only a few channels can be expected to present observable resonances or slightly bound states. Among them, we have found that the $D\overline{D}^*$ system must show a bound state slightly below the threshold for charmed mesons production with quantum numbers $J^{PC}(I) = 1^{++}(0)$, that could correspond to the widely discussed $X(3872)$. Out of the systems made of a particle and its corresponding antiparticle, $D\overline{D}$ and $D^*\overline{D}^*$, the $J^{PC}(I) = 0^{++}(0)$ is attractive. For the $D^*\overline{D}^*$ the attraction is stronger and structures may be observed close and above the charmed meson production threshold. Also, we have shown that the $J^{PC}(I) = 2^{++}(1)$ $D^*\overline{D}^*$ channel is attractive and may then represent a charge state contributing to charmonium spestroscopy. Due to heavy quark symmetry, the replacement of the charm quarks by bottom quarks decreases the kinetic energy without significantly changing the potential energy. In consequence, four-quark bottomonium mesons must also exist and have larger binding energies.

We have seen how the $4q1\overline{q}$ components, in the form of S wave meson-baryon channels which we identify, play an essential role in the description of the anomalies, say baryon resonances very significantly overpredicted by three-quark models based on two-body interactions. As a matter of fact by considering a simplified description of the anomalies as systems composed of a free meson-baryon channel interacting with a three-quark confined

component we have shown they could correspond mostly to meson-baryon states but with a non-negligible $3q$ state probability which makes their masses to be below the meson-baryon threshold. The remarkable agreement of our results with data in all cases takes us to refine our definition and propose the dominance of meson-baryon components as the signature of an anomaly. Though it is probable that these results may vary quantitatively when a more complete dynamical coupled-channel calculation is carried out we think it is reasonable not to expect major qualitative changes.

We also presented results for the two and three-baryon systems with strangeness -1. We have solved the Faddeev equations for the ΛNN and ΣNN systems using the hyperon-nucleon and nucleon-nucleon interactions derived from a chiral constituent quark model with full inclusion of the $\Lambda \leftrightarrow \Sigma$ conversion and taking into account all three-body configurations with S and D wave components. In the case of the ΛNN system the inclusion of the three-body D wave components increases the attraction, reducing the upper limit of the $a_{1/2,1}$ ΛN scattering length if the $(I,J) = (0,3/2)$ ΛNN bound state does not exist. This state shows a somewhat larger sensitivity than the hypertriton to the three-body D waves. Our calculation including the three-body D wave configurations of all relevant observables of two- and three-baryon systems with strangeness -1, permits to constrain the ΛN scattering lengths to: $1.41 \leq a_{1/2,1} \leq 1.58$ fm and $2.33 \leq a_{1/2,0} \leq 2.48$ fm. In the case of the ΣNN system there exists a narrow quasibound state near threshold in the $(I,J) = (1,1/2)$ channel.

We have presented results for the doubly strange $N\Xi$ and $Y_1 Y_2$ interactions ($Y_i = \Sigma, \Lambda$). We showed that the constituent quark model predictions are consistent with the recently obtained doubly strange elastic and inelastic scattering cross sections. In particular, our results are compatible with the $\Xi^- p \to \Lambda\Lambda$ conversion cross section, important in assessing the stability of Ξ^- quasi-particle states in nuclei.

It is expected that in the coming years better-quality data on all sectors discussed in this talk will become available and our results can be used to analyze these upcoming data in a model-independent way.

VI. ACKNOWLEDGMENTS

This work has been partially funded by the Spanish Ministerio de Educación y Ciencia and EU FEDER under Contracts No. FPA2007-65748 and FPA2010-21750, by Junta de Castilla y León under Contract No. GR12, and by the Spanish Consolider-Ingenio 2010 Program CPAN (CSD2007-00042),

[1] A. Valcarce, H. Garcilazo, F. Fernández, and P. González, Rep. Prog. Phys. **68** (2005) 965.
[2] N. Isgur and G. Karl, Phys. Tod. Nov. 1983 (1983) 36.
[3] E. Eichten, K. Gottfried, T. Kinoshita, K. D. Lane, and T. -M. Yan , Phys. Rev. D **21** (1980) 203.
[4] N. Isgur, Phys. Rev. D **60** (1999) 054013.
[5] E. J. Eichten, K. Lane, and C. Quigg, Phys. Rev. D **69** (2004) 094019.
[6] S. L. Olsen, arXiv:0901.2371 [hep-ph]

[7] R. L. Jaffe, Phys. Rev. D **15** (1977) 267; J. D. Weinstein and N. Isgur, Phys. Rev. D **41** (1990) 2236; G. 't Hooft, G. Isidori, L. Maiani, A. D. Polosa, and V. Riquer, Phys. Lett. B **662** (2008) 424.
[8] H. Pöpping, P. U. Sauer, and X. -Z. Zhang, Nucl. Phys. A **474** (1987) 557; A. Valcarce, F. Fernández, H. Garcilazo, M. T. Peã, and P. U. Sauer Phys. Rev. C **49** (1994) 1799.
[9] F. E. Close, arXiv:0706.2709.
[10] T. Fernández-Caramés, A. Valcarce, and J. Vijande, Phys. Rev. Lett. **103** (2009) 222001.
[11] S. K. Choi *et al.* (Belle Collaboration), Phys. Rev. Lett. **100** (2008) 142001.
[12] R. Mizuk *et al.* (Belle Collaboration), Phys. Rev. D **78** (2008) 072004.
[13] B. Aubert *et al.* (BaBar Collaboration), Phys. Rev. D **79** (2009) 112001.
[14] T. Caramés, A. Valcarce, and J. Vijande, Phys. Rev. D. **82** (2010) 054032.
[15] P. González, J. Vijande, and A. Valcarce, Phys. Rev. C **77** (2008) 065213.
[16] C. Amsler *et al.* [Particle Data Group], Phys. Lett. B **667** (2008) 1.
[17] S. Capstick and N. Isgur, Phys. Rev. D **34** (1986) 2809.
[18] D. M. Manley and E. M. Saleski, Phys. Rev. D **45** (1992) 4002.
[19] R. E. Cutkosky, C. P. Forsyth, J. B. Babcock, R. L. Kelly, and R. E. Hendrick, Proceedings of the IV International Conference on Baryon Resonances, edited by N. Isgur, Toronto 1980.
[20] A. Valcarce, H. Garcilazo, and J. Vijande, Phys. Rev. C **72** (2005) 025206. J. Vijande, F. Fernández, and A. Valcarce, J. Phys. G **31** (2005) 481.
[21] H. Garcilazo, T. Fernández-Caramés, and A. Valcarce, Phys. Rev. C **75** (2007) 034002.
[22] H. Garcilazo, A. Valcarce, and T. Fernández-Caramés, Phys. Rev. C **76** (2007) 034001.
[23] Y. Fujiwara, Y. Suzuki, and C. Nakamoto, Prog. Part. Nucl. Phys. **58** (2007) 439. Y. Fujiwara, K. Miyagawa, M. Kohno, and Y. Suzuki, Phys. Rev. C **70** (2004) 024001.
[24] A. Deloff, Phys. Rev. C **61** (2000) 024004.
[25] H. Takahashi *et al.*, Phys. Rev. Lett. **87** (2001) 212502.
[26] K. Nakazawa *et al.*, Proceedings of the 10th International Conference on Hypernuclear and Strange Particle Physics (HypX), Tokai (2009).
[27] A. Ichikawa, Ph.D. Thesis, Kyoto University (2001).
[28] E. Hiyama, M. Kamimura, Y. Yamamoto, and T. Motoba, Phys. Rev. Lett. **104** (2010) 212502.
[29] J. K. Ahn *et al.*, Phys. Lett. B **633** (2006) 214.
[30] C. J. Yoon *et al.*, Phys. Rev. C **75** (2007) 022201(R).
[31] T. Nagae *et al.*, J-PARC proposal E05, $http://j-parc.jp/NuclPart/pac_0606/pdf/p05-Nagae.pdf$.
[32] T. Harada, Y. Hirabayashi, and A. Umeya, Phys. Lett. B **690** (2010) 363.
[33] A. Valcarce, H. Garcilazo, and T. F. Caramés, Phys. Lett. B **693** (2010) 305.
[34] T. Tamagawa *et al.*, Nucl. Phys. A **691** (2001) 234c.
[35] Y. Yamamoto, T. Tamagawa, T. Fukuda, and T. Motoba, Prog. Theor. Phys. **106** (2001) 363.
[36] J. K. Ahn *et al.*, Nucl. Phys. A **625** (1997) 231.
[37] S. Aoki *et al.*, Nucl. Phys. A **644** (1998) 365.
[38] C. Nakamoto, Y. Fujiwara, and Y. Suzuki, Nucl. Phys. A **639** (1998) 51c.
[39] H. Polinder, J. Haidenbauer, and U. -G. Meissner, Phys. Lett. B **653** (2007) 29.
[40] V. G. J. Stoks and Th. A. Rijken, Phys. Rev. C **59** (1999) 3009.
[41] Th. A. Rijken and Y. Yamamoto, nucl-th/0608074.
[42] K. Yazaki, Prog. Part. Nucl. Phys. **24** (1990) 353.
[43] Th. A. Rijken and Y. Yamamoto, Phys. Rev. C **73** (2006) 044008.